

Extracellular Vesicle Directed Exogenous Ion Channel Transport for Precise Manipulation of Biological Events

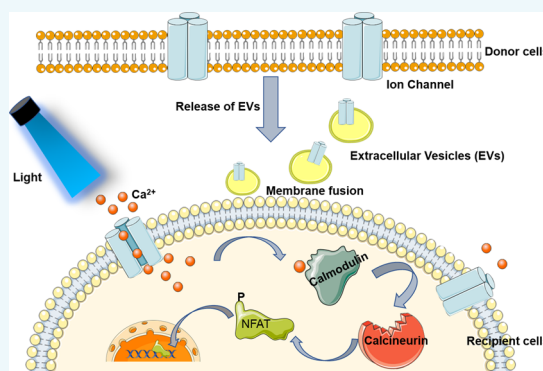
Linna Lyu,[†] Ming Hu,[†] Afu Fu,[§] and Bengang Xing^{*,†}

[†]Division of Chemistry and Biological Chemistry, School of Physical & Mathematical Sciences, Nanyang Technological University, Singapore, 637371

[§]School of Chemical and Biomedical Engineering, Nanyang Technological University, 62 Nanyang Drive, Singapore, 637459

Supporting Information

ABSTRACT: A larger number of human diseases are related to dysregulation or loss of cellular functions. Effective restoration of the missing or defective cellular functions is highly desirable for fundamental research and therapeutic applications. Inspired by the fantastic feature of cell-derived extracellular vesicles (EVs) that can transport various bioactive molecules between cells, herein, we developed a simple and efficient strategy based on EVs for transferring ion channels to recipient cells, thereby conferring specific biological function to the target cells and regulating the biological events. The constructed channel rhodopsin 2 (ChR2)-loaded EV (EV-ChR2) system can mediate the anchor of light-responsive ion channel ChR2 on the plasma membrane of recipient cells through membrane fusion. Upon blue light irradiation, the ion channel ChR2 was activated and opened, thus permitting the rapid flux of cation ions (e.g., calcium ion) across the plasma membrane of recipient cells. Moreover, the increased Ca^{2+} in the cytosol could effectively activate Ca^{2+} -dependent transcription factors, further triggering the calcium signaling pathway. This strategy can be extended to modulate other cellular processes and provides a novel insight on the manipulation of biological events.



INTRODUCTION

The living cell, as a highly complicated and collaborative system, has evolved a wide range of mechanisms to regulate basic physiological processes including proliferation, differentiation, and metabolism.^{1–3} However, dysregulation or loss of cellular functions has been implicated in numerous diseases, such as autoimmunity, cancer, diabetes, neurodegenerative disorders, or cardiovascular disease.^{4–6} Therefore, effective strategies to restore the missing or defective cellular functions or confer specific function to target cells are highly desirable, which not only contribute to comprehensive elucidation of essential physiological processes but also open up novel therapeutic modalities.

Up to now, a myriad of strategies have been developed to recover or bestow specific function on recipient cells. For instance, genetic engineering is one of the commonly used methods for modifying cell functions.^{7–11} Although promising, such a strategy does not allow for the dose- and time-controlled expression of the exogenous protein.¹² Moreover, the exogenous gene and viral vectors have the potential to integrate into endogenous genes, resulting in undesirable immune responses and toxicity.^{13–15} Another popular approach is the introduction of bioactive proteins to target cells. In general, proteins with a specific biological function are directly transported to living cells via an artificial carrier.^{16,17} Compared with genetic engineering, direct protein delivery is

easier to control and possesses lower risk of permanent cell damage. Despite this, this method generally requires soluble proteins which are obtained through a series of protein preparation steps, including protein expression, purification, and post-modifications.¹⁸ These complicated processes may cause protein inactivation or denaturation. Furthermore, most membrane proteins require a lipid-like environment to maintain their stability and intrinsic activities.^{19,20} These fundamental issues have hindered the practical application of such proteins. Therefore, a simple and innovative strategy that allows introduction of specific functional proteins and, more importantly, precise manipulation of their functions remains a big challenge.

Recently, extracellular vesicles (EVs) have gained significant attention as important mediators of intercellular communication, potential disease biomarkers, and drug carriers.^{21–26} EVs including microvesicles and exosomes are lipid bilayer-enclosed nanovesicles that are released from cells.^{27–29} These cell-derived nanoparticles have been shown to transfer native biological molecules (e.g., mRNAs, siRNAs, microRNAs, and proteins) between cells, thus involved in regulating various physiological and pathological processes, such as

Received: May 31, 2018

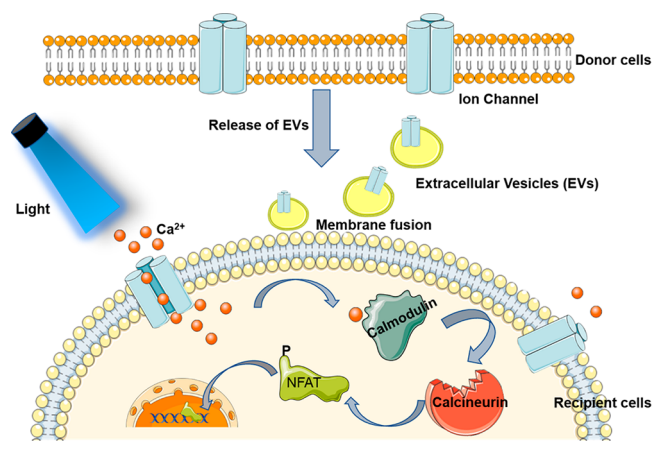
Revised: June 27, 2018

Published: June 28, 2018

cellular homeostasis, blood coagulation, immune regulation, and cancer metastasis.^{30–35} By taking advantage of EVs' intrinsic functions of transmitting biological information between cells, herein, we develop a novel EV-based platform capable of endowing native membrane proteins to target cells, thus enabling precise regulation of related biological events. In this design, EVs act as both the bioactive protein source and transfer carrier. In principle, this strategy exhibits multiple advantages for protein transfer. First, EVs can directly transport original bioactive proteins in intact form from donor cell to recipient cells, which avoids complicated protein extraction and purification. Second, the natural phospholipid bilayers of EVs not only protect the loaded proteins from degradation in blood circulation but also improve the cellular internalization of proteins through direct fusion with the plasma membrane of targeted cells.³⁶ Third, EVs, especially those derived from autologous cells, have been reported to be less immunogenic than synthetic vehicles due to their natural compositions.²⁸ Taken together, these potential advantages make EVs promising for precise modulation of various biological processes.

As a proof of concept, we investigated EV-directed anchor of exogenous ion channels on the plasma membrane of recipient cells for noninvasive regulation of ion influx across the plasma membrane. Ion channels are important membrane proteins, which allow the flow of specific ions and are involved in a large number of cellular processes.³⁷ In this study, a light-gated ion channel ChR2³⁸ is chosen as mode protein to investigate the feasibility of this novel method. As shown in Scheme 1, natural

Scheme 1. Illustration of EV-Mediated Anchor of Exogenous Ion Channel on the Cell Membrane to Achieve Remote Manipulation of Biological Events



photoreceptive ion channels expressed in donor cells are supposed to be naturally located on the surface of the secreted EVs owing to the cellular originality of EVs. The membrane fusion between EVs and recipient cells may allow direct attachment of these exogenous photoswitchable ion channels on the plasma membrane of recipient cells. Upon blue light irradiation, light-sensitive ion channels could be activated, thus allowing noninvasive regulation of ion (e.g., Ca²⁺) influx across the plasma membrane in living cells. Most importantly, the increased Ca²⁺ in cytosol could also activate Ca²⁺-dependent transcription factors (e.g., NFAT, nuclear factor of activated T cells), thus achieving control of calcium signaling.³⁹

RESULTS AND DISCUSSION

Preparation and Characterization of EV-ChR2 Vesicles. To prepare extracellular vesicles with the desired ChR2 protein (EV-ChR2), we first transfected donor cells HEK293T with a plasmid encoding ChR2 protein. The expression of ChR2 on the plasma membrane of donor cells was confirmed by the presence of the green fluorescent protein marker (Venus) using confocal microscopy and flow cytometry. As shown in Figure 1A, after transfection for 3 days, the obvious green fluorescence from Venus reporter was visualized on the donor cell membrane, which colocalized well with the red fluorescence from commercial cell membrane stain (CM5K-Cy5). In contrast, the control cells displayed no detectable fluorescence on the plasma membrane, demonstrating the successful expression of ChR2-Venus on the HEK 293T cell membrane. Moreover, flow cytometry analysis (Figure 1B,C) further confirmed that both the Venus mean fluorescence intensity and the percentage of ChR2-Venus-containing cells were significantly higher than those untreated cells, suggesting a high expression level of ChR2-Venus protein in transfected HEK 293T cells.

The ChR2-loaded EVs were then isolated from culture supernatants of transfected donor cells through differential centrifugation. As controls, supernatants were obtained from untreated HEK293T cells. Transmission electron microscopy (TEM) imaging revealed that both EV and EV-ChR2 were round in shape, and dynamic light scattering (DLS) analysis showed that the size distribution of vesicles was from 100 to 1000 nm (Figure 2A). In addition, the presence of ChR2 proteins on EVs secreted from transfected HEK293T cells was confirmed by monitoring the fluorescence signals of Venus reporter using confocal microscope and flow cytometry. As presented in Figure 2B, there was remarkable green fluorescence observed in EV-ChR2 group. Moreover, the fluorescence signals were visualized on the surface of the EVs. As control, the EVs isolated from normal HEK293T cells displayed negligible fluorescence, indicating that the recombinant protein ChR2-Venus was loaded on the surface of EVs during the production of EVs. Furthermore, the flow cytometry analysis demonstrated that EV-ChR2 vesicles exhibited higher fluorescence intensity than the control group (Figure 2C and D). All these results confirmed the presence of ion channel ChR2 on EVs released by transfected HEK293T cells.

Evaluation of the Transfer of Ion Channel ChR2. To investigate the possibility that exogenous ion channel could be anchored in recipient cells through EVs, we used confocal microscopy to monitor the presence of ChR2-Venus in the cells for several hours following EV-ChR2 vesicle treatment. As presented in Figure 3, after 1 h of incubation, there was weak green fluorescence observed in A549 cells, indicating that there were few ChR2 proteins attached on the cell surface. Under prolonged cellular incubation (e.g., 2 and 4 h), the green fluorescent signals become stronger and obvious green fluorescence was visualized on the surface of recipient cells after 4 h treatment, suggesting that the majority of ChR2-Venus proteins were anchored on the plasma membrane of A549 cells. In contrast, there was negligible signal observed in A549 cells with treatment of control EVs (Figure S1). Similar results were also observed in NIH 3T3 recipient cells (Figure S2). In addition, flow cytometry confirmed that EV-ChR2-treated A549 cells displayed enhanced fluorescent signals

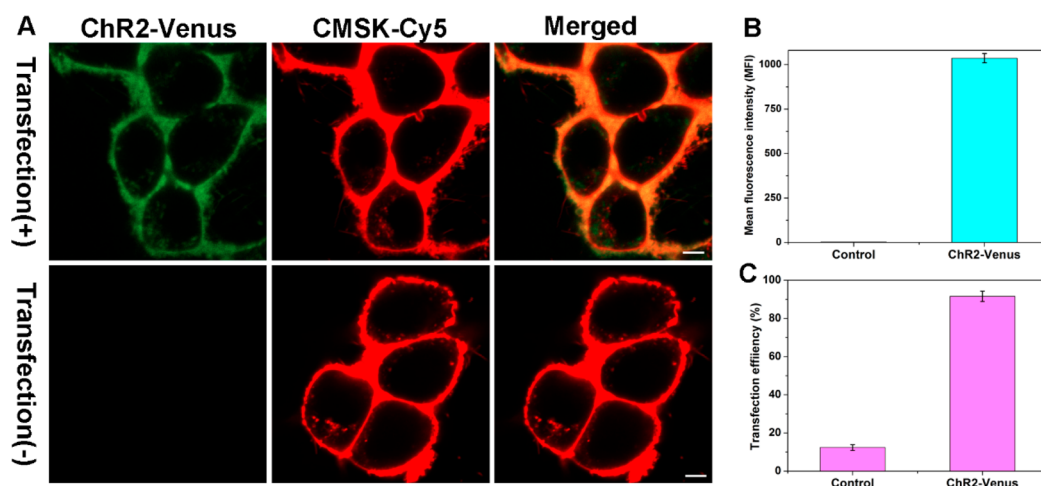


Figure 1. Characterization of transfected donor cells HEK 293T. (A) Confocal imaging of transfected HEK293T cells stained with cell membrane dye. Untransfected cells were control group. Green: ChR2-Venus (E_x : 488 nm, E_m : 500–550 nm), red: CMSK-Cy5 (E_x : 640 nm, E_m : 650–700 nm). Scar bar: 5 μm . (B) Quantitative analysis of fluorescence intensity of HEK293T cells expressing ChR2-Venus by flow cytometry, untransfected cells as control (E_x : 488 nm, E_m : 525/50 nm). (C) Quantitative flow cytometric analysis of transfection efficiency of pCAGGS-ChR2-Venus plasmid in HEK293T cells, untransfected cells as control. (E_x : 488 nm, E_m : 525/50 nm).

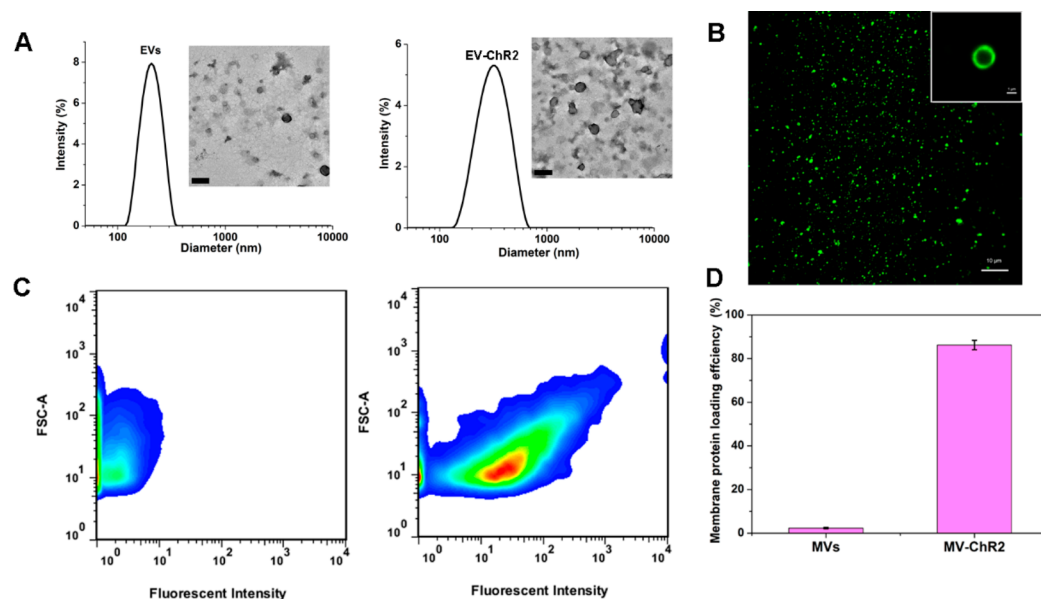


Figure 2. Preparation and characterization of EV-ChR2 generated from transfected HEK293T cells. (A) Size distribution and TEM images of EV and EV-ChR2, scar bar: 300 nm. (B) Confocal images of EV-ChR2, scar bar: 10 μm . Insert: representative confocal image of single EV-ChR2 vesicle, scar bar: 1 μm (E_x : 488 nm, E_m : 525–630 nm). (C) Flow cytometry analysis of EVs and EV-ChR2 (E_x : 488 nm, E_m : 525/50 nm). (D) Quantitative analysis of ChR2-Venus membrane protein loading efficiency (E_x : 488 nm, E_m : 525/50 nm).

compared to EV-incubated cells (Figure S3). This evidence clearly suggested that an exogenous ion channel could be incorporated into the plasma membrane of recipient cells by natural vesicles. Moreover, the EV-ChR2 vesicles were biocompatible and did not cause obvious cytotoxicity against A549 cells, even at high concentration (Figure S4).

Evaluation of the Function of Anchored ChR2 in Vitro. Next, we investigated the function of ChR2 anchored in recipient cells, which is capable of allowing the influx of cation ions such as Ca^{2+} across the plasma membrane under blue light irradiation. To visualize the dynamic changes of Ca^{2+} ions in recipient cells, a calcium indicator (Rhod-3 AM), was used to measure the level of intracellular Ca^{2+} ions. As shown in Figure 4a,b, blue light irradiation of A549 cells preincubated with EV-ChR2 vesicles could result in remarkable enhancement of red

fluorescence in the cytoplasm, while there was no obvious fluorescence change in control experiments for recipient cells treated with EVs (Figure 4c,d). Confocal images clearly demonstrated that the exogenous ChR2 channel could be effectively activated under blue light irradiation and in turn regulate calcium ion influx from the extracellular space.

Moreover, calcium signals play a vital role in diverse physiological processes including cell migration, proliferation, differentiation, and gene transcription.³⁹ To this end, we further investigated the ability of anchored exogenous ion channel to mediate Ca^{2+} -dependent NFAT (nuclear factor of activated T cells) translocation. Typically, NFAT factors with phosphorylated form reside in the cytoplasm of resting cells; following an increase in intracellular Ca^{2+} level, they are dephosphorylated by phosphatase calcineurin. Then, NFAT

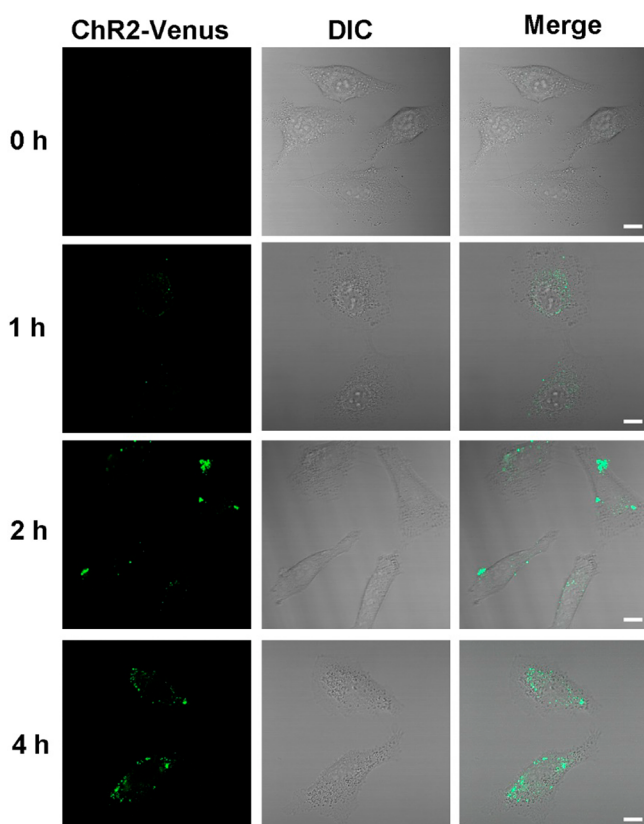


Figure 3. Confocal images of A549 cells incubated with EV-ChR2 for different times. Green: ChR2-Venus (E_x : 488 nm, E_m : 525–600 nm). Scar bar: 10 μm .

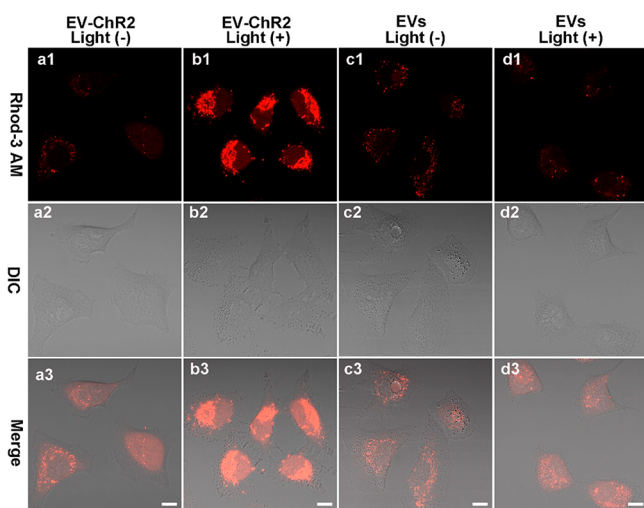


Figure 4. Intracellular Ca^{2+} imaging of EV-ChR2-treated A549 cells in the absence (a) or presence (b) of blue light irradiation (~ 480 nm, 10 min). Intracellular Ca^{2+} imaging of EVs-treated A549 cells in the absence (c) or presence (d) of blue light irradiation (~ 480 nm, 10 min). E_x : 561 nm, E_m : 576–700 nm. Scar bar: 10 μm .

proteins translocate to the nucleus and initiate a variety of gene transcription.^{40–42} Therefore, NFAT possesses a remarkable capability to sense the oscillatory changes of intracellular Ca^{2+} concentration and offer a link between calcium signaling and gene transcription. We examined the Ca^{2+} -dependent nuclear translocation of NFAT by performing antiNFAT2 immunostaining after different treatments. As shown in Figure 5a, EV-

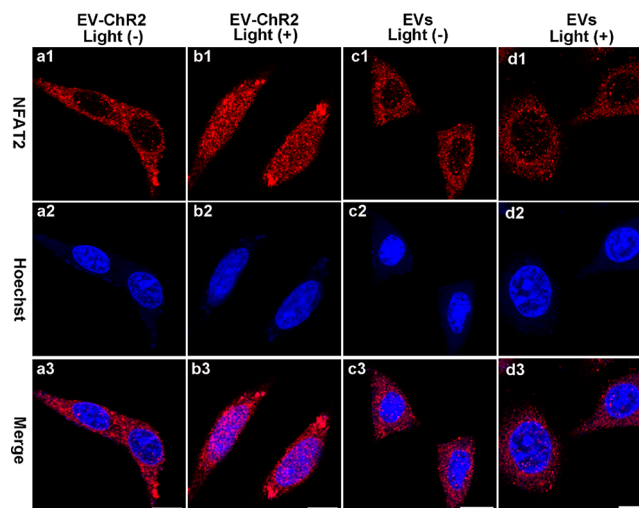


Figure 5. Immunofluorescence imaging of NFAT2 in EV-ChR2-treated A549 cells without blue light irradiation (a) and with blue light irradiation (~ 480 nm, 20 min, 5 min break after 5 min irradiation) (b). Immunofluorescence imaging of NFAT2 in EV-treated A549 cells without blue light irradiation (c) and with blue light irradiation (~ 480 nm, 20 min, 5 min break after 5 min irradiation) (d). Red: antiNFAT2 (E_x : 640 nm, E_m : 576–700 nm), blue: Hoechst 33258 (E_x : 405 nm, E_m : 410–470 nm). Scar bar: 10 μm .

ChR2-treated recipient cells presented an obvious red fluorescence in the cytosol, revealing that NFAT2 was located in the cytoplasm. Upon blue light illumination, EV-ChR2-treated cells exhibited an increase in red fluorescence in the nuclear region, indicating NFAT2 factors translated from the cytosol to the nucleus. In control experiments, there was no apparent fluorescence enhancement visualized in the nucleus of EV-incubated cells under light irradiation (Figure 5c,d). In addition, the blue light irradiation did not lead to obvious cytotoxicity (Figure S5) and cell apoptosis (Figure S6) at the experimental condition. These results further suggested that natural extracellular vesicles could serve as an effective platform for transfer of natural ion channel to remotely regulate calcium signaling.

Evaluation of the Function of Anchored ChR2 in Vivo. To further test whether EV-transferred ChR2 could regulate calcium signaling in vivo, we used fluorescence microscopy to monitor the oscillatory change of Ca^{2+} ions in zebrafish. Typically, we implanted recipient cells with calcium indicator (Rhod-3 AM) into the yolk sac of zebrafish larvae at 48 h post-fertilization (hpf). Subsequently, we injected EV-ChR2 vesicles into the yolk sac of zebrafish larvae to enable effective anchoring of ChR2 channels onto the plasma membrane of recipient cells in the abdominal cavity of the larvae. The bright green fluorescence in the larvae abdomen suggested the successful injection of vesicles in zebrafish (Figure 6). We then utilized blue light to irradiate the larvae and monitor the calcium influx in zebrafish through observing the fluorescence of calcium indicator. As shown in Figure 6, after blue light irradiation for 20 min, an obvious fluorescent enhancement was observed in the zebrafish that have been injected with EV-ChR2 vesicles, while there is little fluorescence change detected in the zebrafish treated with EV Vesicles (Figure S7). These results clearly indicated that extracellular vesicles could remotely regulate calcium signaling in vivo by rendering ChR2 ion channels.

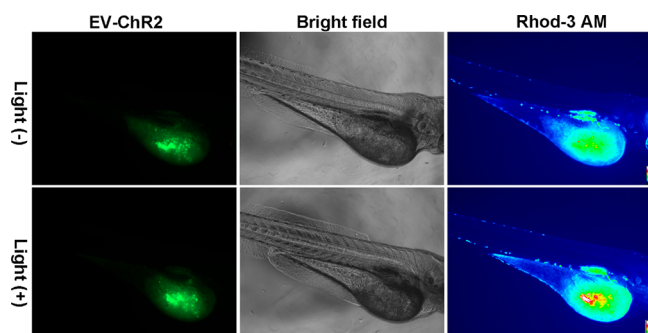


Figure 6. In vivo fluorescence imaging with and without blue light treatment (4.5 mW cm^{-2} for 30 min) in zebrafish incubated with EV-Chr2 ($n = 10$). The Ca^{2+} response in fish was monitored by Rhod-3 AM and analyzed with pseudocolored imaging. Green: Chr2-Venus (E_x : 488 nm, E_m : 500–550 nm), yellow and pseudocolor: Rhod-3 AM (E_x : 561 nm, E_m : 590–670 nm).

CONCLUSIONS

In summary, we have exploited a novel strategy based on natural EVs to selectively confer specific biological function to target cells. The constructed EV-Chr2 system could effectively anchor the exogenous light activated ion channel on the recipient cell membrane. Upon blue light irradiation, the ion channel can be activated, which allowed calcium ion influx. Moreover, the intracellular calcium signaling of modified recipient cells can be invasively regulated. This strategy provided a new insight on precise regulation of target cells and holds great potential for biomedical research and therapeutic applications.

MATERIALS AND METHODS

Materials. Dulbecco's modified Eagle medium (DMEM), fetal bovine serum (FBS), phosphate buffered saline (PBS), penicillin-streptomycin (100 \times), trypsin-EDTA, Opti-MEM, PureLink HiPure plasmid DNA purification kit, Lipofectamine 3000 transfection kit, Cell Mask deep red plasma membrane stain, and Rhod-3 calcium imaging kit were purchased from Thermo Fisher Scientific. Hoechst 33258 was obtained from Sigma. Anti-NFAT2 antibody and Goat Anti-Mouse IgG H&L (Alexa Fluor 647) were purchased from Abcam. All the commercially reagents were used as received unless otherwise noted.

Instruments. The centrifugation was performed on Sorvall LYNXTM 6000 superspeed centrifuge. Transmission electron microscopy (TEM) images were taken on a FEI EM208S transmission electron microscope (Philips) operated at 100 kV. The size distribution of the EVs was examined by Zetasizer Nano ZSP (Malvern Instruments, NK). Confocal imaging of cells was recorded on Carl Zeiss LSM 800 confocal laser microscope (Germany). Fluorescence imaging of zebrafish was carried out on Carl Zeiss fluorescence microscope. Flow cytometry (FACS) was conducted with a Fortessa x 20 instrument (BD Company). Photoirradiation experiments were performed with a fiber optical illuminator (EINST Technology Pte Ltd.).

Cell Culture. Human embryonic kidney 293T (HEK 293T) cells, human lung carcinoma A549 cell lines, and mouse embryo fibroblast cell line NIH3T3 were purchased from American Type Culture Collection (ATCC). All cells were maintained in Dulbecco's modified Eagle medium (DMEM) supplemented with 100 $\mu\text{g}/\text{mL}$ streptomycin, 100 units/mL

penicillin, and 10% FBS. All cell lines were cultured in an incubator with 5% CO_2 at 37 $^\circ\text{C}$.

Transient Transfection. The plasmid (pCAGGS-Chr2-Venus) encoding Channelrhodopsin2-Venus was obtained from Addgene. This commercial plasmid (in *E. coli*) was expanded and purified using plasmid midiprep kit by following the standard protocol. For transient transfection, HEK 293T cells were seeded in a 75 cm^2 flask or 3.5 cm dish until 80% confluence. The culture medium was replaced with serum-free MEM medium. The commercial Lipofectamine 3000 (Invitrogen) was used as transfection reagent by following the manufacturer's protocol. After 4 h incubation, the medium with transfection reagent was replaced with fresh cell culture medium and the cells were continually cultured for another 48 h. The Chr2-Venus expression was confirmed by confocal laser scanning microscopy and flow cytometry. For confocal imaging, the cells in 3.5 cm dish were washed with DMEM medium for two times and stained with CellMask Deep Red Plasma Membrane Stain (5 μM) for 10 min. The images were taken on Carl Zeiss LSM 800 confocal microscope. (Chr2-Venus: $E_x = 488 \text{ nm}$, $E_m = 500\text{--}550 \text{ nm}$), cell membrane stain: $E_x = 640 \text{ nm}$, $E_m = 650\text{--}700 \text{ nm}$). For quantification of Chr2-Venus on the cell membrane, the collected transfected cells were resuspended in 0.5 mL cold PBS. The suspensions were analyzed with BD LSR Fortessa x 20 flow cytometer (E_x : 488 nm, E_m : 525/50 nm). The mean fluorescence was measured by counting 10 000 cells.

Extracellular Vesicle (EV) Isolation. EVs were isolated and purified from the supernatants of transfected cells or untreated cells by differential centrifugation, according to previous studies. In brief, the cells expressing Chr2-Venus or untreated cells were cultured in serum-free medium for 24 h to allow EVs release. Then, the supernatants were collected and centrifuged for 20 min at 2000 g to get rid of cells and cell debris, followed by centrifugation at 8000 g for 5 min to remove apoptotic bodies. Subsequently, the EVs pellets were formed by centrifugation of supernatants at 60 000 g for 60 min. The obtained EVs were redispersed in sterile PBS and centrifuged again for 60 min at 60 000 g. Finally, the purified EVs were dissolved in PBS and used freshly or stored at $-80 \text{ }^\circ\text{C}$ refrigerator until further use. All the purification procedures were conducted at 4 $^\circ\text{C}$. To quantify the amount of MVs, the total protein content was measured by using a BCA protein assay kit (Bio-Rad).

Characterizations of EVs. The size distribution of prepared vesicles was characterized by Zetasizer Nano ZSP (Malvern Instruments, UK) equipped with a laser (633 nm), at a fixed angle of 173 $^\circ$ and temperature of 25 $^\circ\text{C}$. The data were analyzed using software provided by the instrument. The morphology of EVs was characterized by TEM. Briefly, the EV pellets were fixed with 4% paraformaldehyde in PBS at room temperature for 2 h. After washing with water, the sample solutions were dropped onto a copper grid coated with carbon and stained with 1% phosphotungstic acid. Samples were performed on a FEI EM208S transmission electron microscope (Philips) at 100 kV. To confirm the expression of the Chr2-Venus proteins on the engineered EVs membrane, confocal images were taken by Carl Zeiss LSM 800 microscope. The fluorescent protein Venus was used as reporter. (E_x : 488 nm, E_m : 525–630 nm). To quantify the loading efficiency of Chr2-Venus proteins on the membrane of MVs, suspensions containing EV-Chr2 were analyzed with BD LSR Fortessa x

20 flow cytometer (E_x : 488 nm, E_m : 525/50 nm). EVs without Chr2 were used as control.

Analysis of the Transfer of Chr2 Proteins. For confocal imaging studies, A549 cells were seeded in 3.5 cm ibidi dish at a density of 10^4 cells per well. After 24 h, the cells were washed with PBS and treated with 20 μg of EVs or EV-Chr2 for the indicated times. Confocal images for each group were captured using Carl Zeiss LSM 800 microscope (E_x : 488 nm, E_m : 525–620 nm). For flow cytometry analysis, the A549 cells were seeded in 12-well plate at a density of 1×10^5 cells per well for 24 h. After 4 h incubation with EVs or EV-Chr2, the cells were harvested with 0.25% trypsin-EDTA and re-suspended in 0.5 mL PBS for FCM analysis by BD LSR Fortessa X-20 cell analyzer (E_x : 488 nm, E_m : 525/50 nm).

Calcium Influx Assay. Intracellular calcium concentration was measured using a Rhod 3 calcium imaging kit (Life Technologies) according to the manufacturer's protocol with some modification. In brief, A549 cells were seeded in 4 well chamber at a density of 10 000 cells per well for 24 h, followed by incubation with 20 μg of EVs or EV-Chr2 for 4 h. Subsequently, the cells were washed with DMEM medium three times and incubated with Rhod-3 AM (10 μM) in the dark at 37 °C. After 1 h, the cells were washed with DMEM medium for two times and irradiated with a blue light (~ 480 nm, 4.5 mW cm^{-2}) for 10 min. The cytosolic calcium signals were captured with Carl Zeiss LSM 800 microscope (E_x : 561 nm, E_m : 576–700 nm).

Immunocytochemistry. A549 cells were seeded in 3.5 cm ibidi dish at the concentration of 5×10^4 cells/mL for 24 h. Cells were incubated with 20 μg of EVs or EV-Chr2 at 37 °C for 4 h. Then, the cells were washed with medium three times and irradiated with a blue light (~ 480 nm, 4.5 mW cm^{-2}) for 20 min (5 min break after 5 min irradiation). Subsequently, the cells were washed with ice-cold PBS and fixed with ice-cold methanol for 10 min. After incubation with 0.1% Triton X-100 for 5 min, cells were blocked with 5% BSA (bovine serum albumin) in PBS at 37 °C for 30 min. Cells were incubated with anti-NFAT2 antibody at 4 °C for 12 h and then stained with Alexa Fluor 647-conjugated anti-mouse IgG antibody. The cell nucleus was stained with Hoechst 33258. The subcellular localization of NFAT was visualized with Carl Zeiss LSM 800 microscope. (Hoechst: E_x = 405 nm, E_m = 410–470 nm; Alexa Fluor 647: E_x = 640 nm, E_m = 656–700 nm).

Cell Viability Assay. Generally, the A549 cells were seeded into 96-well plates with a density of 6.0×10^3 cells per well in 100 mL of DMEM with 10% FBS and incubated at 37 °C and 5% CO_2 for 24 h. For EV-Chr2 incubation experiments, the cells were treated with different concentrations of EV-Chr2 for 24 h. Subsequently, vesicle-containing medium was replaced with fresh culture medium and cell viability tests were performed. In the cell-based phototoxicity tests, cells were irradiated with blue light (~ 480 nm) at different time intervals, followed by 24 h incubation and cell viability tests. The cytotoxicity was evaluated by the standard Tox-8 assay. The fluorescence intensity was measured at 590 nm with excitation at 560 nm by using a Tecan Infinite M200 microplate reader. All experiments were repeated three times to obtain the average values.

Cell Apoptosis Measurement. The cell apoptosis was tested by using a standard Annexin V-Cy3 apoptosis detection kit. Briefly, the A549 cells (1×10^5 cells per dish) were irradiated with blue light at the dosage of 4.5 mW cm^{-2} for 20 min (5 min break after 5 min irradiation). After 24 h incubation, the

cell samples were washed with PBS solution and 1 \times annexin-binding buffer, respectively, followed by incubating with 0.5 mL binding buffer containing 5 μL Annexin V-Cy3 solutions ($100 \mu\text{g mL}^{-1}$) for 15 min at room temperature. After washing with buffer solution, the cells were imaged at Carl Zeiss LSM 800 confocal laser microscope. In the control group, the cells without light irradiation were treated and imaged following the above methods.

In Vivo Studies. All animal experimental procedures were performed in compliance with the approved guidelines of the Institutional Animal Care and Use Committee (IACUC) at Nanyang Technological University. Briefly, the purchased embryos were raised with standard E3 medium containing 5 mM NaCl, 0.17 mM KCl, 0.33 mM CaCl_2 , 0.33 mM MgSO_4 , and 0.1% Methylene Blue, pH 7.0–7.2. The embryos were kept in a 28.5 °C incubator after removing the unfertilized embryos and debris in culture dishes. The zebrafish larvae were anesthetized with 0.003% tricaine in E3 medium at 48 h post fertilization (hpf). The recipient cells preincubated with Rhod 3 were harvested at a concentration of 5×10^6 cells/mL and loaded into a borosilicate glass needle pulled by a P97 Flaming/Brown micropipette puller (Sutter Instrument). The recipient cells were implanted into the yolk sac of each zebrafish larvae in a single injection by using an electronically regulated air-pressure microinjector (MPPI-3, Applied Scientific Instrumentation, USA). After cell implantation, the larvae were washed twice with E3 medium and examined for the presence of cells in the yolk sac. The living larvae were then injected with EV-Chr2 vesicles or EVs-DiO and incubated in E3 medium for 2 h. For calcium imaging experiments in vivo, individual zebrafish larvae were anesthetized and stayed in a confocal dish (35 mm, plastic bottom). The blue light treatment (480 nm) for the zebrafish was performed at the dosage of 4.5 mW cm^{-2} for 30 min. The fluorescence imaging in living larvae were recorded before and after 480 nm blue light irradiation by using a Leica MZ6 modular stereomicroscope.

■ ASSOCIATED CONTENT

📄 Supporting Information

The Supporting Information is available free of charge on the ACS Publications website at DOI: 10.1021/acs.bioconjchem.8b00377.

Confocal images; Flow cytometry analysis; Cell viability assay; Live-cell apoptosis imaging after blue light irradiation; In vivo fluorescence imaging with and without blue light treatment (PDF)

■ AUTHOR INFORMATION

Corresponding Author

*E-mail: bengang@ntu.edu.sg.

ORCID

Bengang Xing: 0000-0002-8391-1234

Notes

The authors declare no competing financial interest.

■ ACKNOWLEDGMENTS

This work was partially supported by NTU-AIT-MUV NAM/16001, RG110/16 (S), (RG 35/15) NTU-JSPS JRP grant (M4082175.110), and Merlion 2017 program (M408110000) awarded in Nanyang Technological University (NTU) and

National Natural Science Foundation of China (NSFC) (No. 51628201).

REFERENCES

- (1) Rotty, J. D., Wu, C., and Bear, J. E. (2013) New insights into the regulation and cellular functions of the ARP2/3 complex. *Nat. Rev. Mol. Cell Biol.* 14, 7–12.
- (2) Bray, S. J. (2016) Notch signalling in context. *Nat. Rev. Mol. Cell Biol.* 17, 722–735.
- (3) Pommier, Y., Sun, Y., Huang, S. N., and Nitiss, J. L. (2016) Roles of eukaryotic topoisomerases in transcription, replication and genomic stability. *Nat. Rev. Mol. Cell Biol.* 17, 703–721.
- (4) Simons, M., Gordon, E., and Claesson-Welsh, L. (2016) Mechanisms and regulation of endothelial VEGF receptor signalling. *Nat. Rev. Mol. Cell Biol.* 17, 611–625.
- (5) Cerezo, D., Ruiz-Alcaraz, A. J., Lencina-Guardiola, M., Canovas, M., Garcia-Penarrubia, P., Martinez-Lopez, I., and Martin-Orozco, E. (2017) Attenuated JNK signaling in multidrug-resistant leukemic cells. Dual role of MAPK in cell survival. *Cell. Signalling* 30, 162–170.
- (6) Weinlich, R., Oberst, A., Beere, H. M., and Green, D. R. (2017) Necroptosis in development, inflammation and disease. *Nat. Rev. Mol. Cell Biol.* 18, 127–136.
- (7) Fenno, L., Yizhar, O., and Deisseroth, K. (2011) The development and application of optogenetics. *Annu. Rev. Neurosci.* 34, 389–412.
- (8) Piatkevich, K. D., Subach, F. V., and Verkhusha, V. V. (2013) Engineering of bacterial phytochromes for near-infrared imaging, sensing, and light-control in mammals. *Chem. Soc. Rev.* 42, 3441–3452.
- (9) Tischer, D., and Weiner, O. D. (2014) Illuminating cell signalling with optogenetic tools. *Nat. Rev. Mol. Cell Biol.* 15, 551–558.
- (10) Lopes, R., Korkmaz, G., and Agami, R. (2016) Applying CRISPR-Cas9 tools to identify and characterize transcriptional enhancers. *Nat. Rev. Mol. Cell Biol.* 17, 597–604.
- (11) Carrasco-Ramiro, F., Peiro-Pastor, R., and Aguado, B. (2017) Human genomics projects and precision medicine. *Gene Ther.* 24, 551–561.
- (12) Glorioso, J. C., and Lemoine, N. (2017) Gene therapy-from small beginnings to where we are now. *Gene Ther.* 24, 495–496.
- (13) Dave, U. P., Jenkins, N. A., and Copeland, N. G. (2004) Gene therapy insertional mutagenesis insights. *Science* 303, 333–333.
- (14) Sadelain, M. (2004) Insertional oncogenesis in gene therapy: how much of a risk? *Gene Ther.* 11, 569–573.
- (15) Wu, C., and Dunbar, C. E. (2011) Stem cell gene therapy: the risks of insertional mutagenesis and approaches to minimize genotoxicity. *Front. Med. S.* 356–371.
- (16) Lee, K., Rafi, M., Wang, X., Aran, K., Feng, X., Lo Sterzo, C., Tang, R., Lingampalli, N., Kim, H. J., and Murthy, N. (2015) In vivo delivery of transcription factors with multifunctional oligonucleotides. *Nat. Mater.* 14, 701–706.
- (17) Zuris, J. A., Thompson, D. B., Shu, Y., Guilinger, J. P., Bessen, J. L., Hu, J. H., Maeder, M. L., Joung, J. K., Chen, Z. Y., and Liu, D. R. (2015) Cationic lipid-mediated delivery of proteins enables efficient protein-based genome editing in vitro and in vivo. *Nat. Biotechnol.* 33, 73–80.
- (18) Chica, R. A. (2015) Protein engineering in the 21st century. *Protein Sci.* 24, 431–433.
- (19) Scott, D. J., Kummer, L., Tremmel, D., and Pluckthun, A. (2013) Stabilizing membrane proteins through protein engineering. *Curr. Opin. Chem. Biol.* 17, 427–435.
- (20) Simms, J., and Booth, P. J. (2013) Membrane proteins by accident or design. *Curr. Opin. Chem. Biol.* 17, 976–981.
- (21) Alvarez-Erviti, L., Seow, Y., Yin, H., Betts, C., Lakkhal, S., and Wood, M. J. (2011) Delivery of siRNA to the mouse brain by systemic injection of targeted exosomes. *Nat. Biotechnol.* 29, 341–345.
- (22) Tang, K., Zhang, Y., Zhang, H., Xu, P., Liu, J., Ma, J., Lv, M., Li, D., Katirai, F., Shen, G. X., et al. (2012) Delivery of chemotherapeutic drugs in tumour cell-derived microparticles. *Nat. Commun.* 3, 1282.
- (23) Qi, H., Liu, C., Long, L., Ren, Y., Zhang, S., Chang, X., Qian, X., Jia, H., Zhao, J., Sun, J., et al. (2016) Blood Exosomes Endowed with Magnetic and Targeting Properties for Cancer Therapy. *ACS Nano* 10, 3323–3333.
- (24) Vader, P., Mol, E. A., Pasterkamp, G., and Schifflers, R. M. (2016) Extracellular vesicles for drug delivery. *Adv. Drug Delivery Rev.* 106, 148–156.
- (25) Zhang, H., Deng, T., Liu, R., Bai, M., Zhou, L., Wang, X., Li, S., Wang, X., Yang, H., Li, J., et al. (2017) Exosome-delivered EGFR regulates liver microenvironment to promote gastric cancer liver metastasis. *Nat. Commun.* 8, 15016.
- (26) Yim, N., Ryu, S. W., Choi, K., Lee, K. R., Lee, S., Choi, H., Kim, J., Shaker, M. R., Sun, W., Park, J. H., et al. (2016) Exosome engineering for efficient intracellular delivery of soluble proteins using optically reversible protein-protein interaction module. *Nat. Commun.* 7, 12277.
- (27) El Andaloussi, S., Mager, I., Breakefield, X. O., and Wood, M. J. (2013) Extracellular vesicles: biology and emerging therapeutic opportunities. *Nat. Rev. Drug Discovery* 12, 347–357.
- (28) Fuhrmann, G., Herrmann, I. K., and Stevens, M. M. (2015) Cell-derived vesicles for drug therapy and diagnostics: opportunities and challenges. *Nano Today* 10, 397–409.
- (29) Fernandez-Trillo, F., Grover, L. M., Stephenson-Brown, A., Harrison, P., and Mendes, P. M. (2017) Vesicles in Nature and the Laboratory: Elucidation of Their Biological Properties and Synthesis of Increasingly Complex Synthetic Vesicles. *Angew. Chem., Int. Ed.* 56, 3142–3160.
- (30) Cai, J., Han, Y., Ren, H., Chen, C., He, D., Zhou, L., Eisner, G. M., Asico, L. D., Jose, P. A., and Zeng, C. (2013) Extracellular vesicle-mediated transfer of donor genomic DNA to recipient cells is a novel mechanism for genetic influence between cells. *J. Mol. Cell Biol.* 5, 227–238.
- (31) Skog, J., Wurdinger, T., van Rijn, S., Meijer, D. H., Gainche, L., Curry, W. T., Jr., Carter, B. S., Krichevsky, A. M., and Breakefield, X. O. (2008) Glioblastoma microvesicles transport RNA and proteins that promote tumour growth and provide diagnostic biomarkers. *Nat. Cell Biol.* 10, 1470–1476.
- (32) Buzas, E. I., Gyorgy, B., Nagy, G., Falus, A., and Gay, S. (2014) Emerging role of extracellular vesicles in inflammatory diseases. *Nat. Rev. Rheumatol.* 10, 356–364.
- (33) Robbins, P. D., and Morelli, A. E. (2014) Regulation of immune responses by extracellular vesicles. *Nat. Rev. Immunol.* 14, 195–208.
- (34) Takahashi, A., Okada, R., Nagao, K., Kawamata, Y., Hanyu, A., Yoshimoto, S., Takasugi, M., Watanabe, S., Kanemaki, M. T., Obuse, C., et al. (2017) Exosomes maintain cellular homeostasis by excreting harmful DNA from cells. *Nat. Commun.* 8, 15287.
- (35) van Niel, G., D'Angelo, G., and Raposo, G. (2018) Shedding light on the cell biology of extracellular vesicles. *Nat. Rev. Mol. Cell Biol.* 19, 213–228.
- (36) Sun, D., Zhuang, X., Zhang, S., Deng, Z. B., Grizzle, W., Miller, D., and Zhang, H. G. (2013) Exosomes are endogenous nanoparticles that can deliver biological information between cells. *Adv. Drug Delivery Rev.* 65, 342–347.
- (37) Feske, S., Wulff, H., and Skolnik, E. Y. (2015) Ion channels in innate and adaptive immunity. *Annu. Rev. Immunol.* 33, 291–353.
- (38) Nagel, G., Szellas, T., Huhn, W., Kateriya, S., Adeishvili, N., Berthold, P., Ollig, D., Hegemann, P., and Bamberg, E. (2003) Channelrhodopsin-2, a directly light-gated cation-selective membrane channel. *Proc. Natl. Acad. Sci. U. S. A.* 100, 13940–13945.
- (39) Berridge, M. J., Bootman, M. D., and Roderick, H. L. (2003) Calcium signalling: dynamics, homeostasis and remodelling. *Nat. Rev. Mol. Cell Biol.* 4, 517–529.
- (40) Macian, F. (2005) NFAT proteins: key regulators of T-cell development and function. *Nat. Rev. Immunol.* 5, 472–484.
- (41) Muller, M. R., and Rao, A. (2010) NFAT, immunity and cancer: a transcription factor comes of age. *Nat. Rev. Immunol.* 10, 645–656.

(42) Soboloff, J., Rothberg, B. S., Madesh, M., and Gill, D. L. (2012) STIM proteins: dynamic calcium signal transducers. *Nat. Rev. Mol. Cell Biol.* 13, 549–565.